Inter-calibration of Metop-A and Metop-B scatterometers using ocean measurements

Anis Elyouncha and Xavier Neyt

Royal Military Academy, Brussels, Belgium

ABSTRACT

We recently developed a method for inter-calibrating spaceborne scatterometers. This method was successfully applied to ERS-1/ERS-2 and Metop-A/ERS-2 C-band scatterometers. The method is based on combining different natural targets (ocean, sea ice and rainforest) and associated geophysical models. In this paper, the inter-calibration method is applied to Metop-A and Metop-B scatterometers data with a focus on the ocean measurements. Additionally, the correction coefficients obtained from the ocean are compared to and validated on other independent targets i.e., rainforest and sea ice. Calibration of the scatterometer over ocean is widely used for monitoring and correction of the backscattering coefficients. The method is based on the assessment of the difference between the measured and the simulated backscatter using NWP winds and Geophysical Model Functions (GMF's) such as CMOD5. The method provides the instrument bias against the GMF. It was found that this bias varies spatially and temporally. This temporal and spatial variation of the bias could lead to discrepancies of up to 0.1 dB, which is significant compared to the calibration accuracy (0.2 dB). This adds to the actual bias (instrument drift) an artificial error which is due to the misfit of the input wind distribution. It is shown that this discrepancy is due to the sensitivity of the GMF to the wind speed distribution and this consequently yields the calibration over ocean to be sensitive to the wind speed distribution. The wind speed distribution variation in time and space is analyzed. The sensitivity of the calibration over the ocean to the wind speed distribution variation is assessed. Finally, a method is proposed to mitigate this variation and thus reduces the misfit error.

Keywords: Scatterometer, Ocean calibration, ASCAT, Metop

1. INTRODUCTION

A scatterometer is a radar designed to measure the radar cross-section or the backscattering coefficient σ^0 of the Earth's surface. In order to determine the wind field (speed and direction), the scatterometer makes measurements from different azimuth angles. The fixed fan beam scatterometers use three antennas called fore, mid and aft with azimuth angles 45°, 90° and 135° relatively to the spacecraft body. The spaceborne scatterometers ASCAT-A and ASCAT-B on-board Metop-A and Metop-B satellites respectively use six antennas, three pointing to the right-hand side and three pointing to the left-hand side. Finally, a Geophysical Model Function (GMF) is used to relate the radar cross section to the wind speed and direction.

The received power is converted to σ0 using the radar equation. This operation requires a precise knowledge of the radar parameters such as antenna gain, receiver gain, transmitted power etc. The difference between the measured backscatter and the true backscatter is due to a misknowledge of these parameters, mainly the antenna gain pattern. Thus, the objective of inter-calibration is to correct this antenna gain pattern.

In a previous work[1] an inter-calibration methodology was introduced. This methodology uses a set of three model-based methods to compute the bias between two scatterometers. The methodology makes use of different natural distributed targets namely, ocean, rainforest and the sea ice. This paper focuses on inter-calibration over ocean. The main underlying assumption is that differences in measured σ_0 are due to differences in the antenna gain. Thus, the bias is a function of incidence angle (elevation angle) or the wind vector cell (WVC) across-track number.

Further author information: (Send correspondence to Anis Elyouncha) E-mail: anis.elyouncha@rma.ac.be, Telephone: +32 2 737 6665, Address: Signal and Image Center, Electrical Engineering Dept, Royal Military Academy, 30 av de la Renaissance, B-1000 Brussels, Belgium

The inter-calibration routine is a two step procedure. Firstly, a cross-comparison of the two sensors is performed from which a bias is computed. Secondly, the sigma noughts of the sensor to be calibrated (here ASCAT-B) are corrected using the bias as inter-calibration coefficients.

The advantage of inter-calibration over the calibration of each scatterometer separately,[2][3] resides in several points. Firstly, the fact that inter-calibration uses temporally and spatially collocated datasets eliminates the error induced by the seasonal variation. This, consequently reduces the required data size to typically one month instead of one year required for separate calibration. The impact of the seasonal change of the wind distribution on the calibration bias will be discussed later. Secondly, the NWP model is regularly updated, these updates result in a slight modification of the wind distribution. Since the inter-calibration bias is a ratio of model biases, any change in the NWP winds would cancel out. Finally, In a separate calibration the correction coefficients are validated on ocean only i.e., the training dataset is used as the test dataset. In the proposed inter-calibration method the correction coefficients are also validated on independent datasets such as the rainforest and sea ice. This cross-validation of the calibration coefficients makes the method more robust.

In the next section, the Metop scatterometers are described. In the third section, the ocean inter-calibration methodology is introduced. Section IV is dedicated to the discussion of the problems related to the bias variation. The results of the inter-comparison are shown in the fifth section. In section VI, the inter-calibration coefficients are applied to ASCAT-B data and the results are discussed. Finally, the conclusions are derived in the last section.

2. METOP SCATTEROMETERS

Metop-A satellite was launched on October 19, 2006 followed by the Metop-B satellite on September 17, 2012. Both fly in the same sun-synchronous polar orbit. Metop-B follows Metop-A with 49 minutes delay in a tandem configuration. The two satellites carry real aperture radars (scatterometers) operating at 5.255 GHz (C-band) using six vertically polarized antennas. The scatterometers ASCAT on-board Metop-A and Metop-B (here called ASCAT-A and ASCAT-B respectively) are very similar to the scatterometers on-board ERS satellites. They are all fixed fan beam C-band scatterometers. Three antennas (for, mid and aft) pointing to the left side (left swath) and three antennas pointing to the right side (right swath). The range of incidence angles is approximately $27 - 53^o$ and $35 - 65^o$ for the mid and side antennas respectively. For further detailed information on ASCAT-A and ASCAT-B see.[4]

Metop scatteromters provide nominal and high resolution products. The nominal and high resolution products are organized in lines of 21 and 42 WVC's respectively which are spaced by 25 km and 12.5 km respectively. In this paper nominal products are used, hence the bias has 21 values in range.

3. INTER-CALIBRATION OVER OCEAN METHODOLOGY

The backscatter triplets $(\sigma_0^{fore}, \sigma_0^{mid}, \sigma_0^{aft})$ measured on the sea lie on a surface of a cone. The mathematical representation of this cone is the C-band Geophysical Model function (GMF)[5]

$$\sigma_0(\theta,V,\phi) = B_0(\theta,V)[1 + B_1(\theta,V)cos\phi + B_2(\theta,V)cos2\phi]^{1.6} \tag{1}$$

where V is the wind speed, ϕ is the wind direction and θ is the incidence angle

If the wind direction is uniform, the backscatter (averaged over all wind directions) depends only on wind speed. We obtain the core of the C-band GMF cone B_0.

The ocean calibration[6] consists in the comparison of the measured backscatter against a simulated backscatter. The simulated backscatter σ_0 is computed using ECMWF Numerical Weather Prediction (NWP) winds and the CMOD5 GMF. The ECMWF winds are used as a reference and are assumed unbiased. In inter-calibration this is not important, because any bias in the NWP winds will cancel out. The measured and simulated σ_0 are transformed into z-space ($z = (\sigma_0)^{0.625}$) as suggested in.[5]

First, the averaged deviation of each scatterometer compared to the CMOD5 model i.e., the model bias β^m, is computed as

$$\beta^m(\theta,b) = E[z^{meas}(\theta,V,\phi)]/E[z^{sim}(\theta,V,\phi)] \tag{2}$$

where z^{meas} and z^{sim} are respectively the measured and simulated backscatter transformed to z space. E represents the averaged z over wind directions and wind speeds.

Second, the bias between the two scatterometers is the ratio of the two model biases

$$\beta(\theta,b) = \beta^{m,A}(\theta,b)/\beta^{m,B}(\theta,b) \qquad (3)$$

where $\beta^{m,A}$ and $\beta^{m,B}$ are the model bias for ASCAT-A and ASCAT-B respectively.

Since ASCAT-A and ASCAT-B have 21 WVC'S in each swath, $\beta(\theta,b)$ is a vector of 21 coefficients for each swath and antenna.

4. BIAS VARIATION

As explained previously the ocean calibration is based in the CMOD GMF model. The GMF is an empirical model, its coefficients are tuned to a certain wind dataset which has a given wind speed Probability Density Function (PDF). This PDF is the optimal, i.e., leads to the smallest bias between the measured and the simulated backscatter. Unfortunately this "optimal" distribution is very difficult to reproduce. For inter-calibration purpose the two datasets are assumed to have the same wind distribution.

It was found[7–9] that the parameters of the wind distribution (mean, standard deviation, skewness and kurtosis) vary geographically and seasonally. For instance[9] studied the ERS scatterometer winds bias against buoys winds. He found that the bias follows a systematic seasonal cycle. The sensitivity of the GMF to the wind distribution results in a variation of the ocean calibration bias. Temporally this variation can be illustrated by the seasonal variation of the bias. The regional variation can be illustrated for instance by the discrepancy between Southern and Northern hemisphere.

The objective of the ocean calibration is the determination of the instrument bias against a reference (here ECMWF NWP winds) or against another instrument when it is used for inter-calibration.[1] An addional (artificial) error might be added to the true antenna gain bias. This error is due to the misfit of the wind distributions, and the larger the misfit the larger is the bias error.

$$\beta^m(\theta,b) = \beta^{ant}(\theta,b)\beta^{misfit}(\theta,b) \qquad (4)$$

where $\beta^{ant}(\theta,b)$ and $\beta^{misfit}(\theta,b)$ are the antenna gain bias and the bias due to the wind distribution misfit respectively.

This misfit might be due to a regional scenario (e.g., ERS-2 after 2003), a large gap in one of the two datasets or to an extreme weather conditions in one of the two datasets. Therefore, when the calibration routine is performed on two different datasets spaced in time/space or both, it may lead to significant discrepancies. This discrepancy can reach 0.1 dB.[10] Note that in inter-calibration we are looking for differences of the order of the standard deviation (0.05 dB).

4.1. Wind speed distribution variation

The sea surface wind speed distribution variation has been previously studied.[7,8,11] In[11] for instance, the GEOS3 altimeter wind speeds were analyzed. A seasonal variation of the wind speed was found over the two hemispheres, with highest winds in winter and lower winds in summer. Moreover, an asymmetry in the summer to winter variation (seasonal cycle amplitude) between the two hemispheres was observed. The seasonal cycle amplitude is larger in the Northern Hemisphere (NH) than Southern Hemisphere (SH). There is roughly a factor 2 between them. Therefore, a global wind speed should also undergo a seasonal cycle (if the data is equally distributed) similar to the NH with lower amplitude.

Figure 1 shows the time series of the daily averaged wind speeds for the scatterometer winds and a linear fit to the time series. The dataset run from March 01 to June 15. Thought the time series is relatively short, a decrease and an increase in the wind speed respectively in NH and SH is clearly noticeable. The same trend was observed in ERS-1 and ERS-2 data. This behavior agrees well with.[11] Moreover, it confirms the asymmetry between the two Hemispheres. Note that the NH slope is steeper than the SH slope. Although, the number of samples in SH is larger than in the NH (more ocean in SH) the global wind still showing a seasonal trend. This suggests that the ocean calibration not only must consider a global wind dataset but also the whole year to average out the seasonal effect. To make things more difficult, inter-annual and decadal variations of the wind speed might also exist. Therefore, using, for instance, the ocean calibration without taking into account the wind speed PDF variation to assess the stability of an instrument is not reliable. Similarly, the method is not reliable for calibration over a regional scenario (e.g., ERS-2 since 2003).
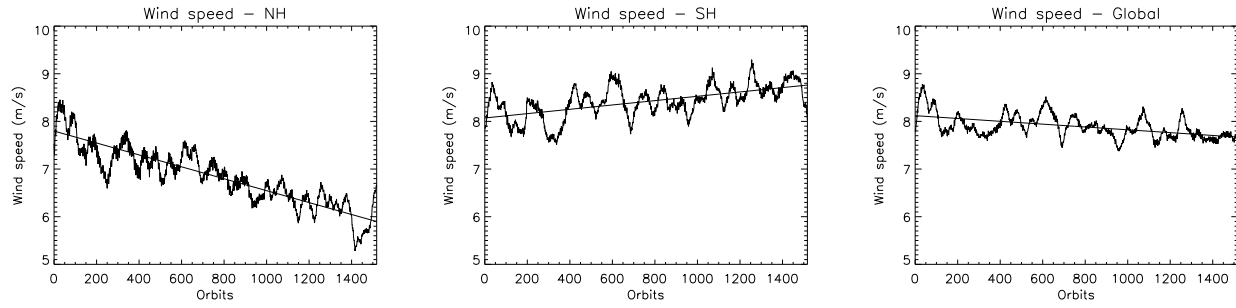
Figure 1. Wind speed time series (from March 01 to June 15), straight line: linear fit, left: Northern Hemisphere, middle: , left: Southern Hemisphere , right: Global

4.2. Impact on the calibration bias

In order to illustrate the regional effect on the model bias, the ocean calibration is analyzed separately for NH and SH. Figure 2 illustrates clearly the difference between the two Hemispheres. The bias is larger when only NH is considered and lower when only SH is considered. Note that the dataset used for ASCAT-A/ASCAT-B corresponds to the NH winter season (January). This correlates with the wind speed variation discussed above. For inter-calibration, this effect has a little impact as long as the same regional dataset is considered for both scatterometers.
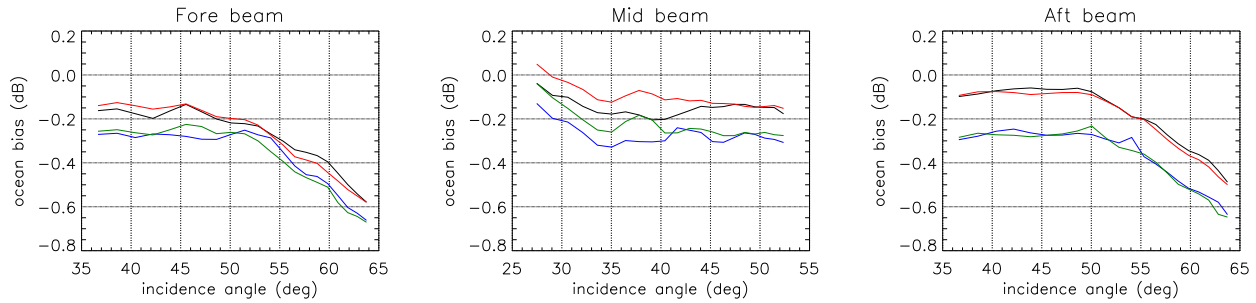

Figure 2. Regional effect on the model bias, Black: ASCAT-A NH, Red: ASCAT-B NH, Blue: ASCAT-A SH, Green: ASCAT-B SH - January 2013

In order to assess the sensitivity of the ocean calibration to the seasonal variation of the wind speed distribution. The dataset (time series) has been divided into four segments consecutive in time. The ocean calibration was applied to each segment, the result is shown in figure 3. The figure illustrates not only the change in the model bias with a changing wind distribution but furthermore it shows that the bias decreases with decreasing wind speed average due to seasonal cycle (see figure 1). This result agrees with[10] such that the bias minima and maxima correspond to summer and winter respectively. Finally, it is worth noting that the seasonal variation of the bias is correlated with the wind speed seasonal variation shown in the previous section. The relationship between the wind and σ_0 might be affected by the seasonal effect. The study of this effect is beyond the scope of this paper.

4.3. Application of rejection sampling method to ocean calibration

In order to mitigate the impact of the wind speed PDF variation on the model bias, rejection sampling method is used to keep this PDF constant. Rejection sampling is a method used to sample from a dataset with certain probability distribution function, such that the selected data will be distributed following a given PDF called the target PDF. This is performed as follows

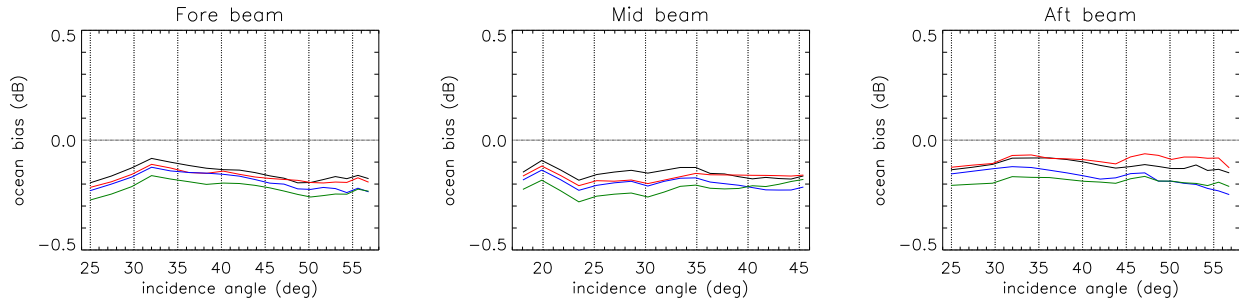- Given a dataset with an empirical distribution $g(x)$

Figure 3. Seasonal effect on the model bias, Black: from 20/3 to 7/4, Red: from 8/4 to 26/4, Blue: from 27/4 to 15/5, Green: from 16/5 to 3/6

- Choose a proposal/target distribution $f(x)$ (with $f < cg$, where $c > 1$)

- Sample randomly x from the data distribution g

- For each sample x, sample uniformly u from $(0, g(x))$

- If the value u is lower than $f(x)$ the sample is accepted else it is rejected

Figure 4 shows three cases (NH, SH and global) of wind distributions. In black are depicted the data histogram, in blue the best Weibull fit. One can notice, these distributions can be significantly different. For instance, the kurtosis is 0.47 for NH, -0.17 for SH and 0.12 for the global distribution. The target distribution is depicted in red, which is the same for the three cases. The red crosses represent the histogram of the selected data, which can be slightly different from the target distribution.
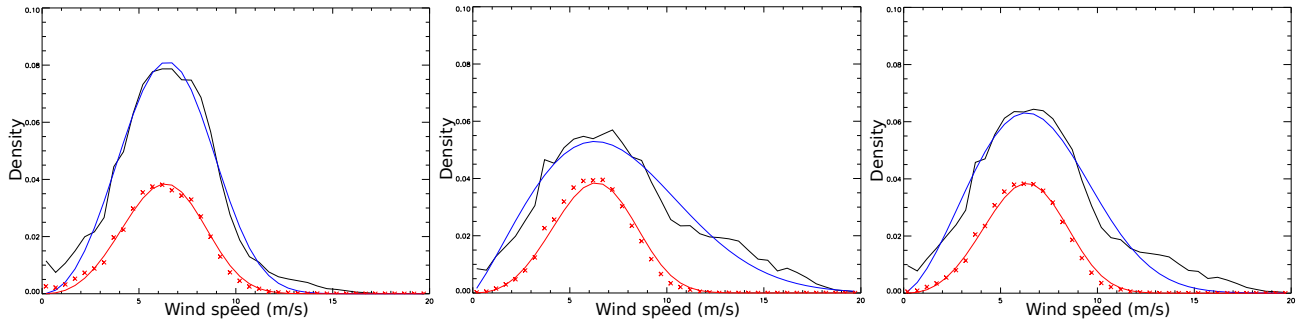

Figure 4. Wind speed distribution, Black: empirical distribution, Blue: best fit, Red-solid: target distribution, Red-cross: histogram of the selected data - left: NH, middle: SH, right: global

Figure 5 depicts the ocean calibration model bias after the application of rejection sampling to the wind speed distributions. These results should be compared with figure 3. First, we notice that though the curves are slightly noisier because data has been filtered out, the discrepancy between the curves has been clearly reduced. Moreover, the degradation of the bias in time is not apparent anymore, i.e., the seasonal effect was removed.

5. INTER-COMPARISON RESULTS

The inter-comparison of ASCAT-A and ASCAT-B is performed on the dataset (between January 01 and January 31 2013) during the tandem mission. Figure 6 shows the inter-comparison bias of ASCAT-A and ASCAT-B for one swath. The cross-comparison bias over rainforest and sea ice are also over-plotted for comparison. Details on how the bias is
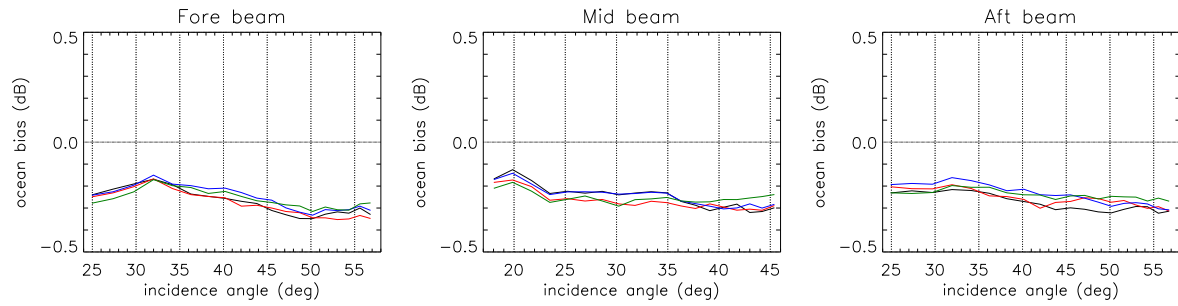
Figure 5. Model bias after rejection sampling, Black: from 20/3 to 7/4, Red: from 8/4 to 26/4, Blue: from 27/4 to 15/5, Green: from 16/5 to 3/6

computed over rainforest and sea ice can be found in.[1] The bias pattern over ocean is very similar to the bias pattern over the other two targets. This indicates that this result is more likely to be related to the antennae gain diagrams. The bias is within 0.09 dB indicating that these two scatterometers are well calibrated. Note that ASCAT-A and ASCAT-B have been cross-calibrated using the rainforest,[12] hence the relatively small differences. Table 1 summarizes the mean bias and standard deviation for the three beams and targets. It will be shown later that this inter-calibration can further be refined.
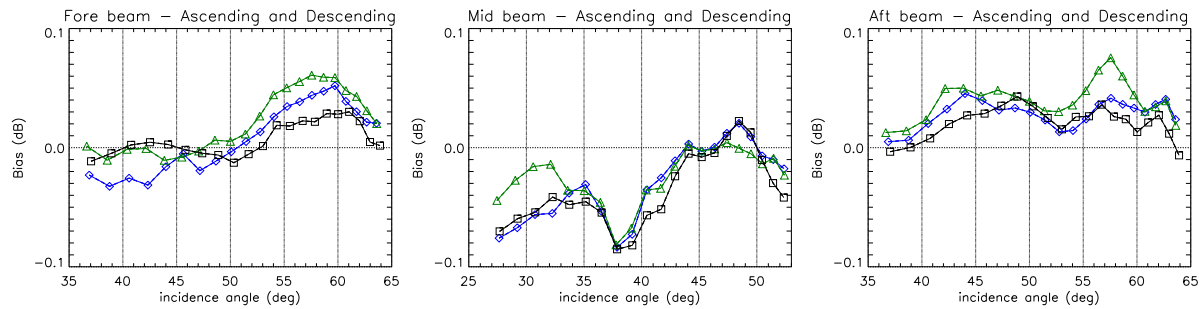

Figure 6. ASCAT-A/ASCAT-B bias - Blue: ocean, Black: sea ice, Green: rainforest - Right swath - Left: Fore beam, middle: Mid beam, right: Aft beam

Beam	Ocean	Rainforest	Sea ice
	Mean bias		
Fore	0.0087	0.0233	0.0076
Mid	-0.0282	-0.0227	-0.0346
Aft	0.0301	0.0384	0.0208
	Standard deviation		
Fore	0.0162	0.0303	0.0267
Mid	0.0148	0.0293	0.0329
Aft	0.0191	0.0277	0.0273

Table 1. ASCAT-A/ASCAT-B inter-comparison - Mean bias and standard deviation (dB)

6. INTER-CALIBRATION RESULTS

In this section, the incidence-angle-dependent coefficients ($\beta(\theta)$) computed from ocean measurements are used to correct the sigma noughts, then the cross-comparison is run again over the three datasets (ocean, sea ice and rainforest). The

residual bias β^{res} (after inter-calibration) is given by

$$\beta^{res}(\theta,b) = \frac{E[z^{meas,A}(\theta,b)/z^{sim,A}(\theta,b)]}{E[(\beta(\theta,b)z^{meas,B}(\theta,b))/z^{sim,B}(\theta,b)]} \tag{5}$$

where $z^{meas,A}$ and $z^{meas,B}$ are the transformed σ^0 measured by ASCAT-A and ASCAT-B respectively.

Each curve on figure 7 shows the residual bias (β^{res}) obtained over a specific target after the application of the ocean inter-calibration coefficients to ASCAT-B data. All the curves are fluctuating around zero with a very small bias within ± 0.03 dB instead of ± 0.09 dB before correction. As expected the ocean bias is the smallest (negligible). Table 2 summarizes the results obtained over the different targets. Generally, the RMS of β^{res} is reduced by two orders of magnitude when the correction is applied to ocean dataset and one order of magnitude when the correction is applied to other datasets. A better correction can be achieved by combining the three targets to minimize the residual bias.
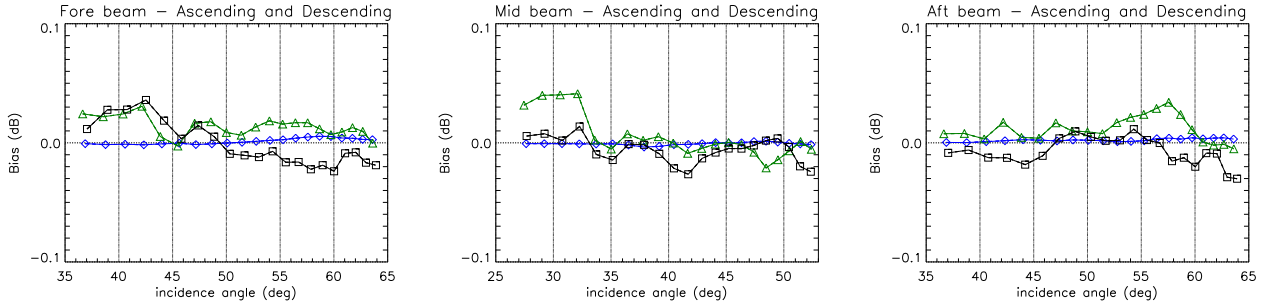

Figure 7. ASCAT-A/ASCAT-B residual bias (after ocean correction), Blue: Ocean, Black: Sea ice , Green: Rainforest - Fore (left), Mid (center), Aft (right) - Ascending and Descending passes - January 2013

Beam	Ocean RMS	RF RMS	Sea ice RMS	Max $|bias_{res}|$
		Before correction		
Fore	0.0096	0.0114	0.0052	0.0608
Mid	0.0139	0.0109	0.0153	-0.0853
Aft	0.0101	0.0142	0.0081	0.0754
		After correction		
Fore	0.0009	0.0052	0.0059	0.0359
Mid	0.0004	0.0060	0.0040	0.0412
Aft	0.0008	0.0051	0.0045	0.0340

Table 2. ASCAT-A/ASCAT-B inter-calibration residual bias - RMS / maximum (dB)

7. CONCLUSIONS

ASCAT-A and ASCAT-B were inter-compared and inter-calibrated using the ocean measurements. The inter-comparison provides that ASCAT-A and ASCAT-B are well calibrated (within 0.1 dB), since they have been previously cross-calibrated. The inter-calibration coefficients derived from the ocean data were validated over other targets. The bias between the two scatterometers was highly attenuated as shown in table 2. The small standard error (≈ 0.03 dB) of the mean bias allows a detection of very small gain drifts. Finally, it was shown that a finer inter-calibration can be achieved using the proposed method which reduces further the residual bias to ≈ 0.03 dB.

ACKNOWLEDGMENTS

REFERENCES

1. A. Elyouncha and X. Neyt, "C-band satellite scatterometer inter-calibration," *IEEE Transactions on Geoscience and Remote Sensing* **51**, pp. 1478–1491, Mar. 2013.

2. J. Verspeek, A. Stoffelen, M. Portabella, H. Bonekamp, C. Anderson, and J. Figa, "Validation and calibration of ASCAT using CMOD5.n," *IEEE Transactions on Geoscience and Remote Sensing* **48**, pp. 386–395, July 2010.

3. J. Verspeek, A. Verhoef, and A. Stoffelen, "ASCAT-B NWP ocean calibration and validation," Tech. Rep. SAF/OSI/CDOP2/KNMI/TEC/RP/199, EUMETSAT, Darmshtadt, 2013.

4. J. Figa-Saldaa, J. Wilson, E. Attema, R. Gelsthorpe, M. Drinkwater, and A. Stoffelen, "The advanced scatterometer (ASCAT) on the meteorological operational (METOP) platform: A follow on for european wind scatterometers," *Can. J. Remote Sensing* **28**(3), p. 404412, 2002.

5. A. Stoffelen, *Scatterometry*. PhD thesis, University of Utrecht, Oct. 1998.

6. A. Stoffelen, "A simple method for calibration of a scatterometer over the ocean," *Journal of atmospheric and oceanic technology* **16**, pp. 275–282, Feb. 1999.

7. A. H. Monahan, "The probability distribution of sea surface wind speeds. part I: Theory and SeaWinds observations," *Journal of Climate* **19**, p. 497520, Feb. 2006.

8. A. H. Monahan, "The probability distribution of sea surface wind speeds. part II: Dataset intercomparison and seasonal variability," *Journal of Climate* **19**, p. 521534, Feb. 2006.

9. Y. Quilfen and B. Chapron, "The ERS scatterometer wind measurement accuracy: evidence of seasonal and regional biases," *Journal of atmospheric and oceanic technology* **18**, pp. 1684–1697, Apr. 2001.

10. J. Verspeek, A. Verhoef, and A. Stoffelen, "ASCAT NWP ocean calibration," Tech. Rep. version 1.5, KNMI/EUMETSAT OSI SAF, KNMI, de Bilt, 2011.

11. D. T. Sandwell and R. W. Agreen, "Seasonal variation in wind speed and sea state from global satellite measurements," *Journal of Geophysical Research: Oceans* **89**, pp. 2041–2051, Mar. 1984.

12. J. Figa-Saldana and C. Anderson, "ASCAT-B level 1 commissioning report," Tech. Rep. EUM/OPS/DOC/12/3436, EUMETSAT, Darmshtadt, 2013.